



Green Synthesis of Silver Nanoparticles Blended with *Citrus Hystrix* Fruit Juice Extract and their Response to Periodontitis Triggering Microbiota

Shivkanya Fuloria^{1*}, Neeraj Kumar Fuloria¹, Choo Jin Yi¹, Tang Mei Khei¹, Tan Ann Joe¹,
Law Tiew Wei¹, Sundram Karupiah¹, Neeraj Paliwal¹, Kathiresan Sathasivam²

¹Pharmaceutical Chemistry Unit, Faculty of Pharmacy, AIMST University, Kedah, 08100 Malaysia

²Department of Biotechnology, Faculty of Applied Sciences, AIMST University, Kedah, 08100 Malaysia

Email: shivani2jaju@gmail.com

ABSTRACT

Evidences over periodontitis predominance by human microbiota, inhibitory response of *Citrus hystrix* against periodontitis triggering bacteria and potentiation of antimicrobial response by silver nanoparticles (SNPs) were the stimulus to perform green synthesis of SNPs blended with *Citrus hystrix* and evaluation against periodontitis triggering microbiota. Present study involved SNPs biosynthesis using *Citrus hystrix* fruit juice extract (CHFJE), optimization (using UV-Visible spectrometry), characterization (by FTIR, FESEM, XRD, and EDX), stability study (by UV-Visible spectrometry), and evaluation of green SNPs against periodontitis triggering microbiota (using well diffusion method). Biogenic SNPs exhibited absorbance signal at 430 nm. Optimization study established 15 mM AgNO₃ concentration, 5:5 CHFJE and AgNO₃ volumetric ratio, pH 7, 60 °C temperature and 60 min time as parametric requirement for green synthesis of SNPs using CHFJE. Stability study exhibited absorbance signal between 428-457 nm supporting SNPs stability. The SNPs biosynthesis success was based on broad and shifted FTIR bands; size below 28 nm in FESEM; XRD signals at 38.95, 44.97, 64.92 and 78.97 representing 111, 200, 220 and 311 planes; and elemental silver 83.66 %, carbon 11.87 % and oxygen 4.47 % in EDX spectrum. SNPs displayed maximum inhibitory zone against *B. cereus* (9.66±0.57 mm and 18 mm), followed by *P. aeruginosa* (8.66±0.57 mm and 18.33±0.57 mm), *E. coli* (8 mm and 17.33±.57 mm) and *S. pyogenes* (6.33±0.57 mm and 13 mm) at 50 µg/mL and 100 µg/mL concentration. Present study establish that green synthesis of SNPs using CHFJE is a facile method and also the SNPs blended with *Citrus hystrix* fruit juice extract (CHFJE) possess high inhibitory potential against periodontitis triggering microbiota.

Keywords: Bionanocomposites, Microflora, Periodontitis, Stability, Optimization

Received 21.04.2019

Revised 04.05.2019

Accepted 16.05. 2019

INTRODUCTION

Studies in recent decade report human microflora to possess 1:1 ratio of bacteria and human cells [1, 2]. An infinitesimal disturbance in the ratio of human microbiota may lead to various infections and diseases [3]. Among all such infections and disease periodontal disease is reported as most complex polymicrobial inflammatory disease. Periodontal disease is interrelated to dysbiosis of dental biofilm that causes chronic inflammation of periodontal lining of soft tissue and results in destruction of tooth and alveolar bone [4]. The pathogenic micro flora and chronic inflammation related to periodontitis leads to progression of several other systemic diseases, such as: respiratory disease [5], chronic kidney disease [6], cancer [7], rheumatoid arthritis [8], obesity [9, 10], diabetes [11], and cardiovascular diseases [12, 13]. A shift in the microbiota content is considered as key factor for periodontitis [14]. Microbiota disturbance may activate *Pseudomonas aeruginosa* (*P. aeruginosa*), *Escherichia coli* (*E. coli*), *Streptococcus pyogenes* (*S. pyogenes*) and *Bacillus cereus* (*B. cereus*) [15-17]. These microorganisms are highly prevalent in periodontal site of periodontitis patients [18]. Periodontitis is considered as the most oral infectious disorder predominated by microorganisms [19]. The extensive administration of conventional antibiotics against several infections results in prolonged treatment, multiple drug resistance (MDR), and high mortality risk. Current decade witnesses enormous research over metallic nanoparticles [20-22]. Among metallic nanocomposites the massive applications of silver nanoparticles (SNPs) to augment

antimicrobials and other biomedicines, always withdraws researcher attention [23-28]. The SNPs act as a powerful weapon against various MDR bacteria like ampicillin-resistant *E. coli*, erythromycin-resistant *S. pyogenes*, *P. aeruginosa* and *B. cereus*. These are the common opportunistic pathogens of human gut microbiota [29, 30]. Metal nanocomposites can be synthesized by several ways, such as: heat evaporation, chemical reduction, electrochemical reduction, and microwave irradiation [31-35]. Synthesis of SNPs by these methods needs surface passivators for prevention of agglomeration. The application of passivators like thiophenol, mercapto acetate, and thiourea in the synthesis of SNPs might pollute the environment [36]. The chemical synthesis of SNPs may cause adsorption of toxic entities on the particles surface, which may manifest in adverse effects on administration. Though SNPs can be produced using numerous methods, yet a method that presents higher environmental safety, economy, non-toxicity, and yield is a serious apprehension [37]. The nanoparticles biosynthesis which involves use of plant material is considered as green, since it does not involve harmful chemicals. The benefits attached with green synthesis such as environmental friendliness, simplicity, cost-effectiveness, stability, and reproducibility justifies the importance of green synthesis of SNPs [37-39].

Investigations suggest anti-biofilm, antivirulence, anti-inflammatory, antitumor, antioxidant and anticholinesterase activity of *Citrus hystrix* [40, 41]. The fruits of traditional herb *Citrus hystrix* (*C. hystrix*) are known to possess various phytoconstituents such as: terpene, terpenoids, glycerolglycolipids, tannins, tocopherols, furanocoumarins and flavonoids and alkaloids [40]. The *C. hystrix* herb is known to aid the dental health. The high potential of *C. hystrix* plant to inhibit bacteria that triggers periodontal disease always draws the investigators attention [42]. The literary facts suggest that potency of traditional herb *C. hystrix* to inhibit periodontal disease triggering bacteria could be augmented by blending it into SNPs (that enjoys nano penetration at cellular level). Hence, the evidences over complex disorders of periodontitis, periodontitis predominance by human microbiota, *C. hystrix* inhibitory response to periodontitis triggering bacteria and benefit of antimicrobial activity potentiation by silver nanoparticles, intended present study to perform green synthesis of silver nanoparticles (SNPs) blended with *C. hystrix* and evaluate against periodontitis triggering microbiota. Present study involved biogenic SNPs optimization, stability, characterization and evaluation of antimicrobial response against *S. pyogenes*, *E. coli*, *B. cereus*, and *P. aeruginosa*, the common pathogenic microbiota that triggers periodontal disease.

MATERIAL AND METHODS

Materials

The SNPs were biosynthesized using *C. hystrix* fruit juice extract (CHFJE). The chemicals like: potassium bromide (KBr), silver nitrate (AgNO_3), sodium hydroxide (NaOH), dimethyl sulfoxide (DMSO) and Muller Hilton agar were procured from Fisher chemicals, Sigma Aldrich, SD Fine, and Hi-Media. The glasswares were cleaned and washed with deionized water, dried at 160 °C for 2 h and plastic ware was autoclaved before initiation of antimicrobial experiment.

CHFJE preparation

Fresh *Citrus hystrix* fruits free of decay or mold were collected from the province of Kulim, Kedah state, Malaysia and washed with running water. The fruits were cut into half with knife. A manual juicer was used to squeeze the juice from fruits. The squeezed juice was filtered through four-fold muslin cloth and then through a filter paper (Whatman no. 1) to offer *Citrus hystrix* fruit juice extracts (CHFJE). The CHFJE was transferred into a sterilized bottle with screw cap, covered with paraffin film and aluminum foil for storage at 8-10°C in a refrigerator. Prepared CHFJE was used for biosynthesis of silver nanoparticles. Experimental procedure was based on reported methods with slight modification [43].

SNPs green synthesis

The green synthesis of SNPs involved addition of 5 mL of 15 mM AgNO_3 solution (prepared by dissolving 0.255 g of AgNO_3 in 100 mL of deionized water) into 5 mL of freshly extracted CHFJE. The mixture was stirred for 2 min and kept at 60 °C for 1 h to undergo reduction. After the AgNO_3 solution was reduced (color change to brown), the resultant solution was centrifuged at 3000 RPM for 10 min (to separate the SNPs). The supernatant layer was discarded to offer crude SNPs. The crude SNPs were further re-washed with deionized water, re-centrifuged (using the same parameters) and finally air dried to yield pure SNPs. Washing and centrifugation processes were repeated 2 to 3 times (using deionized water to remove any adsorbed substance over SNPs surface). The SNPs biosynthesis was based on reported procedure with slight modification [44-46].

UV-Visible analysis

The SNPs green synthesis success was confirmed by UV-Visible spectrometry. The small aliquot of biosynthesized SNPs was diluted in deionized water (1 mL test sample with 4 mL deionized water. The test mixture obtained was subjected to UV-Visible analysis at room temperature to detect the surface

plasmon resonance (SPR) peak. The measurement was made at 400 to 800 nm using Shimadzu U-2800 spectrophotometer running at scanning speed of 300 nm/min. The UV-visible absorption spectrum of SNPs determined the reduction of Ag⁺ ions. The SNPs solution exhibited an SPR peak at 430 nm. The UV visible analysis was conducted according to reported protocol with minor developments [44-46].

Optimization of parameters for SNPs synthesis reaction mixture

The SNPs biosynthesis was optimized based on UV-Visible spectrometric studies over CHFJE and AgNO₃ reaction mixture maintained under different parametric conditions, such as: volumetric ratio of CHFJE to AgNO₃, concentration of silver nitrate, pH, temperature and time required for green synthesis of SNPs. Optimization was conducted as per reported protocols with minor modifications [44-48].

Optimization of SNPs biosynthesis reaction mixture for concentration of AgNO₃

To optimize the biosynthesis of SNPs, the experimental method for green synthesis of SNPs in present study involved preparation of two individual reaction mixtures, maintained in same conditions except for concentration of AgNO₃. The two reaction mixtures were prepared by taking two different concentrations of AgNO₃ (5 mM and 15 mM). The two reaction mixtures were subjected to visual examination (for monitoring of color change from yellow to brown) and UV-Visible spectrometry (for observation of SPR signal in UV-Visible spectrum) to determine the ideal concentration of AgNO₃ required for green synthesis of pure SNPs.

Optimization of SNPs biosynthesis reaction mixture for volumetric ratio of CHFJE to AgNO₃

Optimization of volumetric ratio of CHFJE to AgNO₃ was done according to the method given for green synthesis of SNPs in the present study. The two individual reaction mixtures were prepared and maintained in same conditions except for volumetric ratio of CHFJE to AgNO₃. The reaction mixtures were prepared in two different volumetric ratios of CHFJE to AgNO₃ (2:8 and 5:5). Both reaction mixtures were subjected to visual examination (to observe color change from yellow to brown) and UV-Visible spectrometric analysis (to monitor SPR signal) to determine the ideal concentration of AgNO₃ required for biosynthesis of pure SNPs.

Optimization of SNPs biosynthesis reaction mixture for pH

To optimize the green synthesis of SNPs, the same experimental protocol given for green synthesis of SNPs in present study was followed. Three solution mixtures were prepared and maintained in same conditions except for pH maintained at pH 3, pH 7 and pH 12. The pH of reaction mixtures was adjusted by adding 0.1 N HCl and 0.1 N NaOH. Each one of the three reaction mixtures with different pH was subjected to visual examination (for observation of change in color from yellow to brown) and UV-Visible analysis (for monitoring of SPR peak) to determine the ideal pH required for green synthesis of pure SNPs.

Optimization of SNPs biosynthesis reaction mixture for temperature

In present study the biosynthesis of SNPs was optimized by following the experimental method given for green synthesis of SNPs. The three reaction mixtures were prepared and maintained in same conditions except for temperature 8-10 °C, 25 °C room temperature and 60 °C. The three reaction mixtures maintained on different temperatures were subjected to visual examination (to monitor color change from yellow to brown) and UV-Visible analysis (to observe the SPR signal) to determine the most suitable temperature required for biosynthesis of pure SNPs.

Optimization of SNPs biosynthesis reaction mixture for time

Based on experimental method given for green synthesis of SNPs in present study, the reaction mixture was prepared and maintained in same conditions except for time. The mixture was noticed for completion of reaction at different time intervals that is 0 min, 30 min, and 60 min. After each stated time intervals, the solution mixture was subjected to visual examination (for change in color from yellow to brown) and UV-Visible spectrometric analysis (for observation of SPR signal) to determine the ideal time required for biosynthesis of pure SNPs.

Biosynthesized SNPs stability studies

After optimization of the key parameters for successful biosynthesis of SNPs, the pure biosynthetic SNPs were subjected to stability studies. The SNPs stability was determined on the basis of SPR signal range (340 to 540 nm) in UV-Visible absorption spectrum. The measurements for stability study were made after 1 day, 7 days, 15 days and 30 days. The procedure for stability study was conducted based on reported methods with minor modifications [44,47,48].

Green SNPs characterization

Once the optimization and stability studies of biogenic SNPs were completed, the pure SNPs were subjected to characterization studies mentioned in other research studies [49-52]. Prior to characterization studies, the biosynthesized SNPs were repeatedly washed and centrifuged using deionized water. The repeated washing and centrifugation process was done to avoid interference of unbound residual biochemical entities of CHFJE with characterization data of biogenic SNPs. The

characterization of biogenic SNPs was based on several analytical techniques such as Fourier transformed infrared spectrometry (FTIR), field emission scanning electron microscopy (FESEM), X-ray diffraction (XRD), and Energy-dispersive X-ray (EDX) spectrometry. The formation of green SNPs was determined based on a change in color of the solution, UV-Visible spectrometer (Shimadzu U-2800) and FTIR (PerkinElmer SLE/MS4/29) spectral data. The FESEM measurement was performed to understand the morphology of SNPs using FEI Nova NanoSEM 450. The SNPs crystal nature was determined by observing their XRD pattern using PANalytical X'Pert PRO MRD PW 3040/60 X-Ray diffractometer. The XRD measurement was operated at 40 kV and 40 mA and spectrum was recorded by $\text{CuK}\alpha\beta$ radiation with a wavelength of \AA in the $1.54060\ 2\theta$ range of $10^\circ - 80^\circ$. The EDX measurement was performed using FEI Nova NanoSEM 450 with EDX unit.

Antimicrobial activity of biosynthesized SNPs against periodontitis causing bacteria

The biosynthetic SNPs were evaluated for antimicrobial potential against *P. aeruginosa* (ATCC 10145), *E. coli* (ATCC 10799), *S. pyogenes* (ATCC 19615), and *B. cereus* (ATCC 11774) using well diffusion method. The fresh and pure culture of each bacterial strain was sub cultured over Muller-Hinton (MH) broth at 37°C (previously shaken on a rotary shaker at 200 rpm). The strain of each bacterial culture was uniformly swabbed using sterile cotton over individual MH agar plates. Using gel puncture wells of 6 mm size were drilled on MH agar plates. In each well of MH agar plate, using micropipette were added SNPs (50 $\mu\text{g}/\text{mL}$ and 100 $\mu\text{g}/\text{mL}$), CHFJE (50 $\mu\text{g}/\text{mL}$ and 100 $\mu\text{g}/\text{mL}$), and ciprofloxacin (10 $\mu\text{g}/\text{mL}$) each in a volume of 50 μl . Lastly, the plates were incubated at 37°C for 24 h, and zone of inhibition was measured. The experimental method was based on other investigation studies with minor developments [49].

RESULT AND DISCUSSION

Green synthesis of SNPs

The SNPs green synthesis results were based on visual examination and UV-Visible spectrometric analysis. The stirred reaction mixture of AgNO_3 solution and CHFJE was kept aside for 60 min at 60°C for monitoring of change in color. After 60 min a color change from yellow to brown was observed. The brown color solution, when subjected to UV-Visible spectrometric analysis, resulted in a signal at 430 nm in the UV-Visible absorption spectrum given in figure 1(A), and indicated the formation of SNPs. In figure 1(A) curve 2 exhibited signal at 430 nm for SNPs, whereas curve 1 exhibited no signal for pure CHFJE. The results of present study were authenticated based on their presence of SPR signal within the range of results claimed by other research studies [44,45,47,48,53,54]. The resultant data of present study confirmed the successful green synthesis of silver nanoparticles using CHFJE. The biosynthesis of SNPs occurred, when AgNO_3 was exposed to CHFJE. The visual examination of color change from yellow to brown and absorbance signal at 430 nm in the UV-Visible spectrum given in figure 1(A) confirmed the formation of SNPs and reduction of Ag^+ to Ag^0 . Both color change from yellow to brown and UV-Visible signal at 430 nm were attributed to surface plasmon resonance property, conceivably a result of stimulation of longitudinal plasmon vibrations stimulation [49].

Optimization of parameters for SNPs biosynthesis reaction mixture

The UV-visible analysis assisted optimization study, optimized five key parameters for the biosynthesis of SNPs namely: silver nitrate concentration, the ratio of CHFJE to silver, pH, temperature, and time. In present investigation, the optimization results were validated based on presence of SPR peak within the results range claimed by other standard investigations [44-47, 53, 54].

Optimization of SNPs synthesis reaction mixture for AgNO_3 concentration

The UV-Visible analysis assisted optimization over green synthesis of SNPs based on two concentrations of AgNO_3 (5 mM and 15 mM) as parameter offered a UV-Visible spectrum given in figure 1(B) containing two curves 1 and 2. In figure 1(B) the curve 1 exhibited signal at 430 nm for SNPs, when 15 mM AgNO_3 was used, whereas curve 2 exhibited no signal for SNPs, when 5 mM AgNO_3 was used. Among two curves 1 and 2, an SPR signal at 430 nm was displayed in curve 1, revealing completion of SNPs green synthesis. The figure 1(B) absorption spectrum generated on analysis of SNPs biosynthesis reaction at different AgNO_3 concentrations (5 mM and 15 mM) revealed that 5 mM of AgNO_3 (representing curve 2) was insufficient to formulate SNPs using CHFJE. Whereas, 15 mM of AgNO_3 (representing curve 1) was sufficient enough to produce SNPs exhibiting a signal at 430 nm. Hence, 15 mM of AgNO_3 concentration was considered as optimum for green synthesis of SNPs. The optimization results for AgNO_3 concentration (15 mM) in present study were confirmed by observing the SPR signal range of other research in similar range [44, 47, 54].

Optimization of SNPs biosynthesis reaction mixture for volumetric ratios of CHFJE to AgNO_3

The UV-Visible spectrometry supported optimization study over green synthesis of SNPs based on two volumetric ratios of CHFJE to AgNO_3 (2:8 and 5:5) as parameter generated UV-Visible absorption spectrum given in figure 1(C) containing two curves 1 and 2. Among two curves 1 and 2, an SPR signal at

430 nm was exhibited in curve 1, that indicated completion of SNPs biosynthesis. The figure 1(C) UV-Visible spectrum obtained on examination of SNPs synthesis reaction at different volumetric ratios of CHFJE to AgNO_3 (2:8 and 5:5) revealed that, 2:8 ratio of CHFJE to AgNO_3 (representing curve 2) was inadequate to formulate SNPs. Whereas, 5:5 CHFJE to AgNO_3 (representing curve 1) was ideal to produce SNPs exhibiting a signal at 430 nm. Hence, 5:5 ratio of CHFJE to AgNO_3 was considered as optimum for green synthesis of SNPs. The optimization study results for volumetric ratio of CHFJE and AgNO_3 (5:5) present study were also confirmed by observing the SPR signal range of other research studies [44, 54].

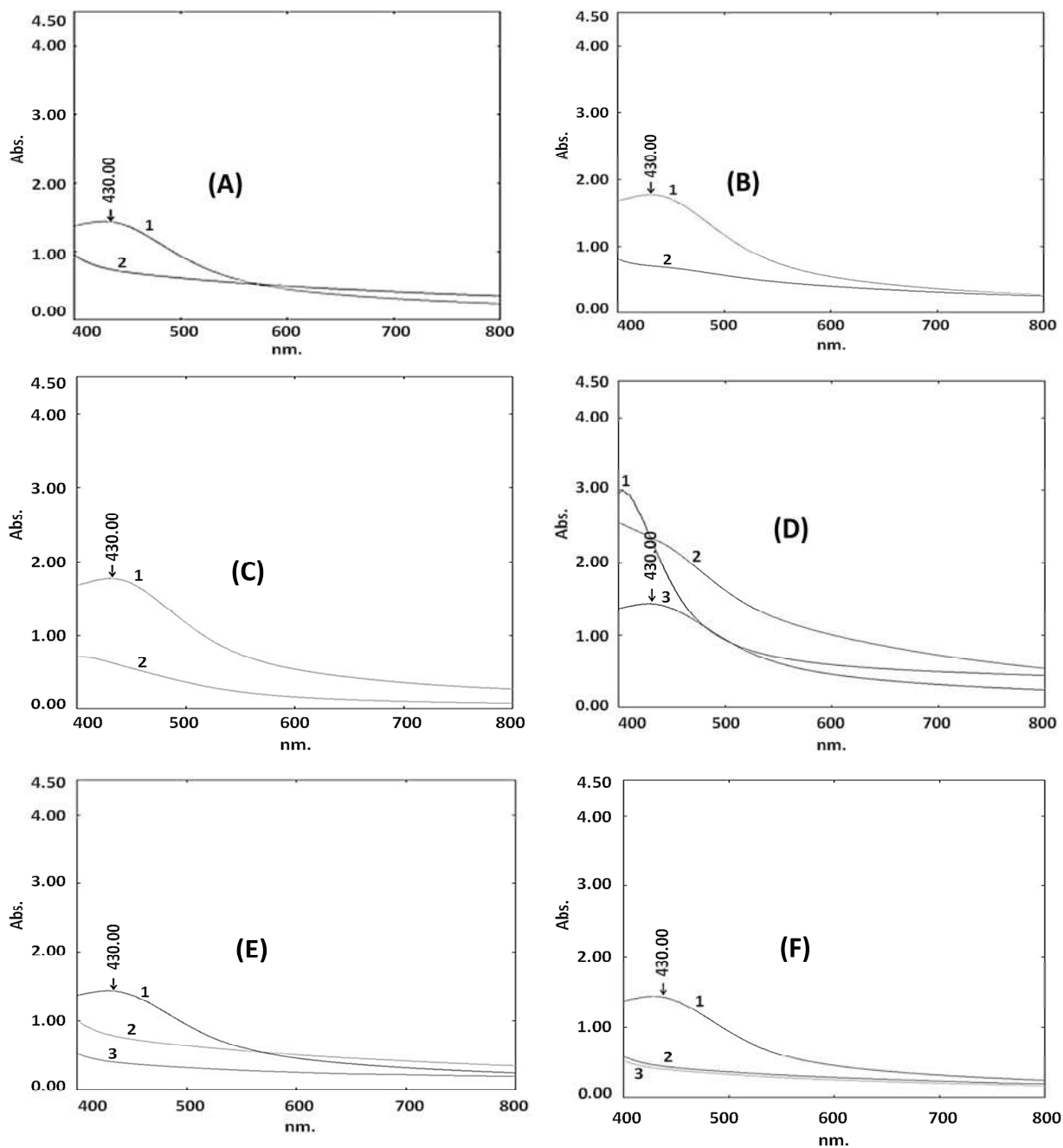


Figure 1: UV-Vis spectra indicating SNPs synthesis (A), Optimization of AgNO_3 concentration (B), Optimization of volumetric ratio of CHFJE ratio to AgNO_3 (C), Optimization of pH (D), Optimization of temperature (E), Optimization of time (F).

Optimization of SNPs synthesis reaction mixture for pH

The UV-Visible experiment aided optimization study over green synthesis of SNPs based on three pH (pH 3, pH 7 and pH 12) yielded a UV-Visible spectrum given in figure 1(D), containing three curves 1, 2 and 3. The UV-Visible spectrum, displayed no absorption signals for SNPs in curve 1 and 2 (related to pH 12 and

pH 7). The spectrum displayed an SPR peak for SNPs in curve 3 (related to pH 3) at 430 nm indicating the completion of green synthesis of SNPs.

The figure 1(D) UV-Visible spectrum produced on analysis of SNPs biosynthetic reaction at different pH (3, 7 and 12) revealed that pH 12 and pH 7 (representing curve 1 and 2) were unsuitable to formulate SNPs. Whereas, pH 3 (representing curve 3) was ideal to produce SNPs displaying signal at 430 nm. Hence, maintaining the reaction at pH 3 was considered as optimum for SNPs biosynthesis. The pH optimization results for biosynthesis of SNPs in present study were verified by observing the similar SPR signal range of other studies [44, 52, 54].

Optimization of SNPs biosynthesis reaction mixture for temperature

The UV-Visible study over SNPs green synthesis based on optimization of temperature (8-10 °C, room temperature and 60 °C) produced a UV-Visible spectrum given in figure 1(E), containing three curves 1, 2 and 3. The figure 1(E) UV-Visible spectrum, displayed no absorption signals for SNPs in curve 2 and 3 (related to room temperature and 8-10 °C). The spectrum displayed an absorption signal for SNPs in curve 1 (related to 60 °C) at 412 nm revealing the completion of green synthesis of SNPs. The absorption spectrum (figure 5) generated during study of SNPs biosynthesis reaction at different temperatures (8-10 °C, room temperature and 60 °C) revealed that, room temperature and 8-10 °C (representing curve 2 and 3) were not ideal to formulate SNPs. Whereas, 60 °C (representing curve 1) was the ideal temperature to produce SNPs displaying signal at 430 nm. Hence, maintaining the reaction at 60 °C was considered as optimum for SNPs green synthesis. The results of optimization study over SNPs green synthesis were also supported by other literary evidences [44, 52, 54].

Optimization of SNPs biosynthesis reaction mixture for time

The UV-Visible analysis over biosynthesis of SNPs based on optimization of time (0 min, 30 min, and 60 min) offered a UV-Visible spectrum given in figure 1(F) containing three curves 1, 2, and 3. The UV-Visible spectrum displayed no absorption signals for SNPs in curve 2, and 3 (30 min and 0 min). The figure 1(F) spectrum displayed an absorption signal for SNPs in curve 1 (related to 60 min) at 430 nm indicating the completion of green synthesis of SNPs. The figure 1(F) UV-visible absorption spectrum obtained while analyzing the SNPs biosynthesis reaction at different time intervals (0 min, 30 min, and 60 min) revealed that duration of 30 min and 0 min (representing curve 2 and 3) were not ideal to formulate SNPs. Whereas, 60 min (representing curve 1) was found ideal time to produce SNPs exhibiting signal at 430 nm. Hence, maintaining the reaction for 60 min of time was considered as optimum for SNPs biosynthesis. The results of optimization study over biosynthesis of SNPs was also supported by other literary evidence [44, 52, 54]

Stability study for biogenic SNPs

The UV-Visible spectrometry assisted in the stability study of green synthesized SNPs. The stability study was conducted for 1 day, 7 days, 15 days, and 30 days. The figure 2 represented, the UV-Visible absorption spectrum of SNPs containing 1, 2, 3, and 4 curves for 1 day, 7 days, 15 days and 30 days respectively. The figure 2, illustrated retention of SNPs signal in the range of 428 to 457 nm. The spectrum illustrated increase in absorbance of green SNPs with time and represented SNPs stability attributed to retention of SNPs signal in the range of 428 to 457 nm. The present study SNPs signal range was also supported by other research studies [44, 52, 54].

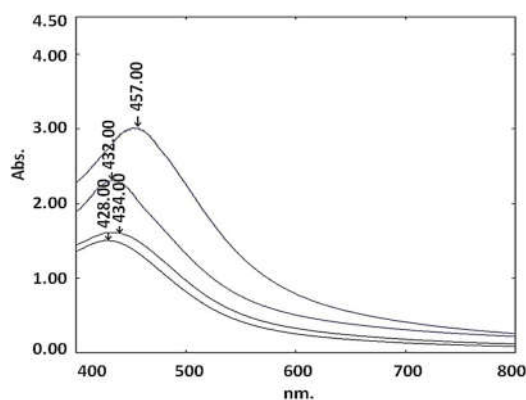


Figure 2: UV-Vis spectrum indicating stability of SNPs

Characterization of green SNPs

Fourier Transformed Infrared (FTIR) analysis

The FTIR characterization study aided in determination of reduction of Ag^+ to Ag^0 and formation of SNPs [54]. The FT-IR spectrum of CHFJE given in figure 3(A), displayed characteristic IR bands at 3402 cm^{-1} (O-

H vibrations), 2930 cm^{-1} and 2870 cm^{-1} (C-H vibrations), 1762 and 1718 cm^{-1} (C=O vibrations), 1550 cm^{-1} (C=N vibrations), 1495 and 1460 cm^{-1} (C=C vibrations). The FTIR spectrum for SNPs given in figure 3(B), displayed shifted bands 3390 cm^{-1} (O-H vibrations), 2912 cm^{-1} and 2869 cm^{-1} (C-H vibrations), 1757 and 1713 cm^{-1} (C=O vibrations), 1542 cm^{-1} (C=N vibrations), 1490 and 1454 cm^{-1} (C=C vibrations). The resultant data indicated the formation of SNPs and the reduction of Ag^+ to Ag^0 [52]. The CHFJE was recognized as a dual capping (stabilizing) and reducing agent based on the comparison of FTIR spectrum of CHFJE and biosynthesized SNPs. The figure 3(B) FTIR spectrum of SNPs was similar to figure 3(B) FTIR spectrum of CHFJE, as it retained the majority of signals with marginal shifting and broadening. For example, 3402 cm^{-1} (O-H vibrations) narrow band in figure 3(A) FTIR spectrum of CHFJE was shifted to 3390 cm^{-1} as a broad band in figure 3(B) FTIR spectrum of SNPs.

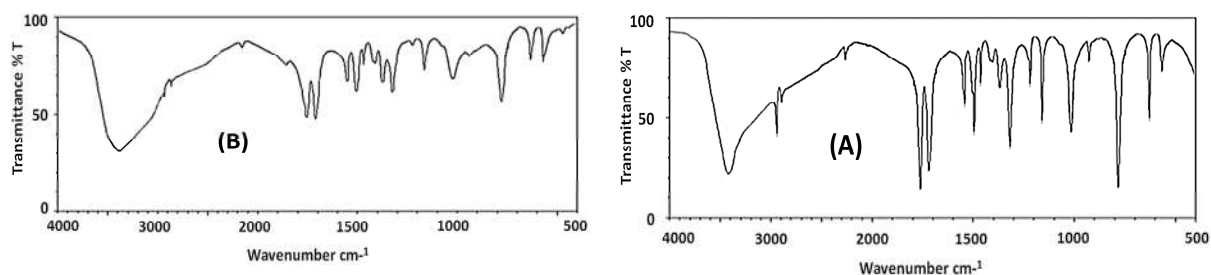


Figure 3: FTIR spectrum of pure CHFJE (A) and biosynthesized SNPs (B).

The literature recorded *Citrus hystrix* fruit juice to possess terpenes (β -pinene, 39.50%), terpinenol (terpinen-4-ol, 17.55%), glycerol-glycolipids, tannins, tocopherols, furano-coumarins, flavonoids and alkaloids [40, 55]. The FTIR spectrum of biogenic SNPs of the present study revealed that the interaction of biochemical moieties of CHFJE with SNPs caused broadening, and marginal shifting of IR band signals positions relatively. This recognized the dual role of CHFJE both as reducing and stabilizing agent [50, 52]. The resultant broadening and shifting of absorption bands in FTIR spectrum of SNPs in comparison to pure CHFJE was also supported by other investigations [47, 52 54].

Field Emission Scanning Electron Microscopy (FESEM)

The FESEM analysis was used to investigate the size and shape of the biosynthetic SNPs [34, 36, 56]. The FESEM micrographs of SNPs (figure 4), indicated that biosynthesized SNPs were well dispersed, spherical shaped, and ranged less than 27.66 nm in size. The FESEM micrograph given in figure 4, epitomized the diverse magnifications and confirmed that biosynthesized SNPs were well dispersed, spherical in shape, crystalline in nature, were smaller than 27.66 nm in size, and were resulted by complete reduction of silver from silver nitrate solution by CHFJE.

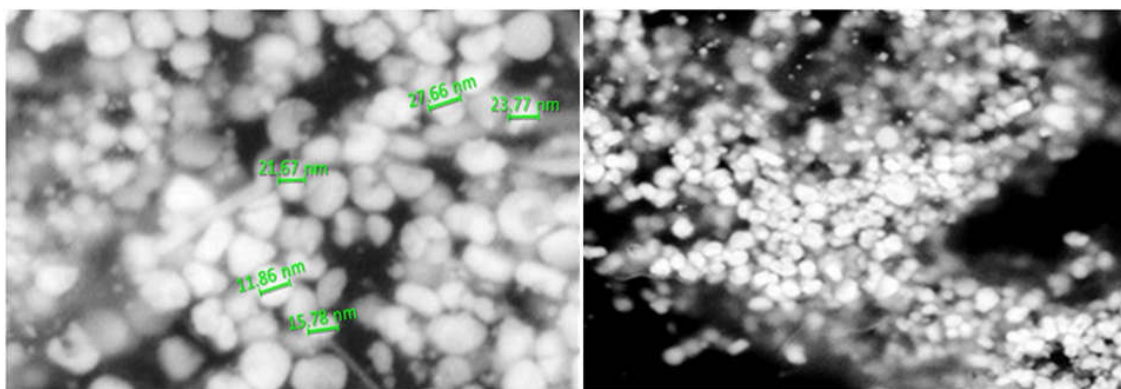


Figure 4: FESEM image of SNPs

X-Ray diffraction (XRD) analysis

Biosynthesized SNPs were characterized using powder XRD analysis to confirm the nanoparticles as silver and to understand the structural information. Crystal nature of biogenic SNPs was confirmed based on analysis of XRD pattern. The analysis of XRD pattern (figure 5) showed the distinctive diffraction peaks at 2θ values of 38.95, 44.97, 64.92 and 78.97 degrees designated to 111, 200, 220 and 311 reflection planes of the face-centered cubic structure of silver. The XRD pattern results of present study were verified by other standard studies [50, 51].

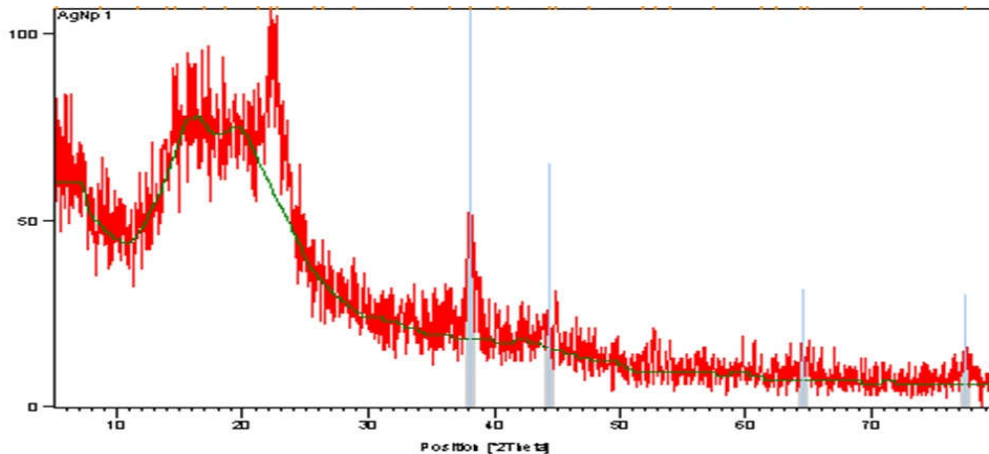


Figure 5: XRD spectrum of SNPs

Energy dispersive X-Ray diffraction (EDX) analysis

To understand the presence of elements involved in SNPs, the EDX study was used to carry out the elemental analysis of SNPs [57]. The EDX spectrum of SNPs (figure 6) exhibited silver (83.66 %) as a major constituent element compared to carbon (11.87 %) and oxygen (4.47 %). Generally, metallic silver nanoparticle shows their typical optical absorption peak approximately at 3 KeV [56]. The EDX spectrum (figure 6) revealed the percentage of silver (83.66 %) as highest in SNPs, followed by carbon (11.87 %), and oxygen (4.47 %). The EDX spectrum showed a strong signal for silver along with weak oxygen peak which may be attributed to the biomolecules that are bound to the surface of silver nanoparticles, indicating the reduction of silver ions to elemental silver [59]. Generally, metallic silver nanoparticle shows their typical optical absorption peak approximately at 3 KeV [58].

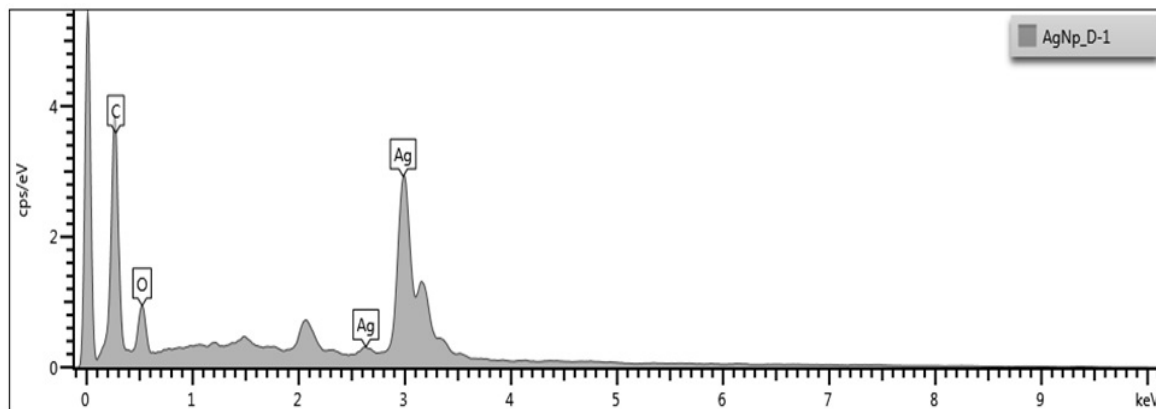


Figure 6: EDX spectrum of SNPs

Antimicrobial activity of SNPs against periodontitis triggering microbiota

Optimized and characterized biogenic SNPs were tested for their inhibition potential against periodontal disorder triggering pathogenic microbiota, the *P. aeruginosa*, *E. coli*, *S. pyogenes* and *B. cereus* (data given in table 1).

The biogenic SNPs presented maximum inhibition zone against *B. cereus* (9.66 ± 0.57 mm and 18 mm), followed by *P. aeruginosa* (8.66 ± 0.57 mm and 18.33 ± 0.57 mm), *E. coli* (8 mm and 17.33 ± 0.57 mm) and *S. pyogenes* (6.33 ± 0.57 mm and 13 mm) in 50 $\mu\text{g}/\text{mL}$ and 100 $\mu\text{g}/\text{mL}$ administered dose. On the other hand, pure CHFJE displayed maximum zone of inhibition against *P. aeruginosa* (6.66 ± 0.57 mm and 11.66 ± 0.57 mm), followed by *B. cereus* (6.33 ± 0.57 mm and 11 mm), *E. coli* (5 mM and 8.66 ± 0.57 mm) and *S. pyogenes* (4 mm and 6.66 ± 0.57 mm) in 50 $\mu\text{g}/\text{mL}$ and 100 $\mu\text{g}/\text{mL}$ concentration. Results of present study were comparable with results of other investigations [19].

The SNPs have extensive use being an antimicrobial and registered as more potent in comparison to silver ions [60]. In the present study, the green SNPs were tested for their response against periodontitis causing pathogenic microbiota namely: *B. cereus*, *P. aeruginosa*, *E. coli*, and *S. pyogenes* using well diffusion method. The resultant data given in table 1, revealed that inhibition zone of green synthesized SNPs was much higher than pure CHFJE. When compared with ciprofloxacin, the newer SNPs exhibited a maximum

zone of inhibition against *B. cereus* (9.66±0.57 mm at 50 µg/mL and 18 mm at 100 µg/mL) and *P. aeruginosa* (8.66±0.57 mm at 50 µg/mL and 18.33±0.57 mm at 100 µg/mL). The SNPs displayed lesser zone of inhibition against *E. coli* (8 mm at 50 µg/mL and 17.33±.57 mm at 100 µg/mL) and *S. pyogenes* (6.33±0.57 mm at 50 µg/mL and 13 mm at 100 µg/mL). In comparison to SNPs, the pure CHFJE exhibited lesser zone of inhibition of against *P. aeruginosa* (6.66±0.57 mm at 50 µg/mL and 11.66±0.57 mm at 100 µg/mL) and *B. cereus* (6.33±0.57 mm at 50 µg/mL and 11 mm at 100 µg/mL). The CHFJE displayed relatively least zone of inhibition against *E. coli* (5 mm at 50 µg/mL and 8.66±0.57 mm at 100 µg/mL) and *S. pyogenes* (4 mm at 50 µg/mL and 6.66±0.57 mm at 100 µg/mL). Interestingly, a pattern was observed in the antimicrobial activity of newer SNPs, when the concentration of SNPs was increased from 50 µl to 100 µl there was a significant increase in the zone of inhibition. The antimicrobial activity results indicated that capping of silver with biochemical moieties of CHFJE (terpenes, terpenols, glycerolglycolipids, tannins, tocopherols, furanocoumarins and flavonoids and alkaloids) caused a marked increase in the antimicrobial potential of SNPs. This pattern of increment in antimicrobial response due to biochemical moieties of plant extract (used for the green synthesis of silver nanoparticles) is also supported by other investigations [52]. The experimental results recognized high antibacterial potential of SNPs (formulated using CHFJE) against periodontitis triggering bacteria, namely: *B. cereus*, *P. aeruginosa*, *E. coli*, and *S. pyogenes*. The antimicrobial results of SNPs (formulated using CHFJE) were comparable to conventional antibiotic (ciprofloxacin). The results of the present study were supported by other investigations also. Other investigations also supported that SNPs smaller in size and higher in dose exhibits higher antimicrobial potential [61-63]

Table 1: Zone of inhibition (expressed in mm ± Standard Deviation)

Microorganism	CHFJE		SNPs		Ciprofloxacin
	50 µg/mL	100 µg/mL	50 µg/mL	100 µg/mL	50 µg/mL
<i>P. aeruginosa</i>	6.66±0.57	11.66±0.57	8.66±0.57	18.33±0.57	21.33±0.57
<i>E. coli</i>	5	8.66±0.57	8	17.33±0.57	20
<i>B. cereus</i>	6.33±0.57	11	9.66±0.57	17	22.66±0.57
<i>S. pyogenes</i>	4	6.66±0.57	6.33±0.57	13	22

As per the pattern of antimicrobial response offered by SNPs against periodontitis triggering pathogens of microbiota (*B. cereus*, *P. aeruginosa*, *E. coli*, and *S. pyogenes*) in present study, it can be hypothesized that small sized SNPs (biosynthesized from CHFJE), when increased in concentration from lower dose (50 µg/mL) to higher dose (100 µg/mL), leads to an increase in antimicrobial response against periodontitis triggering pathogens of microbiota (*E. coli*, *B. cereus*, *S. Pyogenes* and *P. aeruginosa*). Potential of biosynthetic SNPs of present study to inhibit periodontal disorder triggering pathogenic bacteria, was also supported by other studies which supports that plant extract blended SNPs have high potential to inhibit periodontal disease-causing microorganisms [64]. Research evidences accounts *Citrus hystrix* fruits to possess terpenes, terpenols glycerolglycolipids, tannins, tocopherols, furanocoumarins and flavonoids and alkaloids [19]. As per the antimicrobial results of present study and literary evidences it can be postulated that biochemical moieties of CHFJE caused capping of silver and lead to marked increase in antimicrobial potential of SNPs against periodontitis causing pathogenic microbiota.

Present study was a preliminary work on green synthesis of silver nanoparticles from Citrus fruit Juice extract. The study revealed that, silver nanoparticles obtained from Citrus fruit Juice exhibits strong response against *E. coli*, *S. pyogenes*, *P. aeruginosa* and *B. cereus* the human microflora that triggers periodontitis. In future, this method can be employed in drug delivery system as it is a cost effective approach in comparison to other conventional approaches.

CONCLUSION

The visual examination of color change to brown, UV-Vis and FTIR data of the present study confirmed the success of green synthesis of silver nanoparticles using *Citrus hystrix* fruit juice extract (CHFJE). The FESEM, EDX, and XRD data established the morphology of green SNPs with a smaller size than 28 nm, well dispersed, spherical shape, and crystalline nature attributed to complete reduction of silver from silver nitrate solution by CHFJE. The antimicrobial activity of SNPs formulated in present study establish that small sized SNPs (biosynthesized from CHFJE) when increased in concentration from lower dose to higher dose leads to an increase in antimicrobial response. Hence, present study concludes that silver nanoparticles obtained from *Citrus hystrix* fruit juice exhibits strong response against *E. coli*, *S. pyogenes*, *P. aeruginosa* and *B. cereus* the human microflora that triggers periodontitis and recommends Citrus fruit Juice extract as a potential source for green production of potent antimicrobial silver nanoparticles.

ACKNOWLEDGEMENT

Authors are thankful to AIMST University for providing necessary facilities to successfully accomplish this study. Authors are also highly thankful to Nano Optoelectronic Research and Technology (NOR) Lab, School of Physics, Universiti Sains Malaysia for assisting in spectral analysis

CONFLICT OF INTEREST

Authors have no conflict of interest.

REFERENCES

1. Sender, R., Fuchs, S., Milo, R. (2016a). Are we really vastly outnumbered? Revisiting the ratio of bacterial to host cells in humans. *Cell*, 164(3):337–340.
2. Sender, R., Fuchs, S., Milo, R. (2016a). Revised Estimates for the number of human and bacteria cells in the body. *PLoS Biol.*, 14(8):e1002533.
3. Wang, B., Yao, M., Lv, L., Ling, Z., Li, L. (2016). The Human microbiota in health and disease. *Engineering*, 3(1):71–82.
4. Lourenço, T. G. B., Spencer, S. J., Alm, E. J., Colombo, A. P. V. (2018). Defining the gut microbiota in individuals with periodontal diseases: An exploratory study. *J. Oral Microbiol.*, 10(1):1487741.
5. Scannapieco, F. A., Bush, R. B., Paju, S. (2003). Associations between periodontal disease and risk for nosocomial bacterial pneumonia and chronic obstructive pulmonary disease. A systematic review. *Ann. Periodontol.*, 8(1):54–69.
6. Shultis, W. A., Weil, E. J., Looker, H. C., Curtis, J. M., Shlossman, M., Genco, R. J., Knowler, W., Nelson, R. G. (2007). Effect of periodontitis on overt nephropathy and end-stage renal disease in type 2 diabetes. *Diabetes Care*, 30(2):306–311.
7. Ahn, J., Segers, S., Hayes, R. B. (2012). Periodontal disease, *Porphyromonas gingivalis* serum antibody levels and orodigestive cancer mortality. *Carcinogenesis*, 33(5):1055–1058.
8. De Pablo, P., Chapple, I. L., Buckley, C. D., Dietrich, T. (2009). Periodontitis in systemic rheumatic diseases. *Nat. Rev. Rheumatol.*, 5(4):218.
9. Shillitoe, E., Weinstock, R., Kim, T., Simon, H., Planer, J., Noonan, S., Cooney, R. (2012). The oral microflora in obesity and type-2 diabetes. *J. Oral Microbiol.*, 4(1):19013.
10. Keller, A., Rohde, J. F., Raymond, K., Heitmann, B. L. (2015). Association between periodontal disease and overweight and obesity: A systematic review. *J. Periodontol.*, 86(6):766–776.
11. Borgnakke, W. S., Ylostalo, P. V., Taylor, G. W., Genco, R. J. (2013). Effect of periodontal disease on diabetes: Systematic review of epidemiologic observational evidence. *J. Periodontol.*, 84:S135–S152.
12. El Kholy, K., Genco, R. J., Van Dyke, T. E. (2015). Oral Infections and cardiovascular disease. *Trends Endocrin. Metabol.*, 26(6):315–321.
13. Tang W. W., Kitai T., Hazen S. L. (2017). Gut microbiota in cardiovascular health and disease. *Cir. Res.*, 120(7):1183–1196.
14. Berezow A. B., Darveau R. P. (2011). Microbial shift and periodontitis. *Periodontol 2000*, 55(1):36–47.
15. Culotti A., Packman A. I. (2014). *Pseudomonas aeruginosa* promotes *Escherichia coli* biofilm formation in nutrient-limited medium. *PLoS One*, 9(9):e107186.
16. Elshaghabee, F. M., Rokana, N., Gulhane, R. D., Sharma, C., Panwar, H. (2017). Bacillus as potential probiotics: Status, concerns, and future perspectives. *Front. Microbiol.*, 8:1490.
17. Viciani, E., Montagnani, F., Tordini, G., Romano, A., Salerni, L., De Luca, A., Ruggiero, P., Manetti, A. G. (2017). Prevalence of M75 *Streptococcus pyogenes* strains harboring SLAA gene in patients affected by pediatric obstructive sleep apnea syndrome in central Italy. *Front. Microbiol.*, 8:294.
18. Souto, R., Andrade, A. F. B. de, Uzeda, M., Colombo, A. P. V. (2006). Prevalence of "Non-Oral" pathogenic bacteria in subgingival biofilm of subjects with chronic periodontitis. *Braz. J. Microbiol.*, 37(3):208–215.
19. Sudiono, J., Sandra, F., Halim, N. S., Kadrianto, T. A., Melinia, M. (2013). Bactericidal and cytotoxic effects of *erythrina fusca* leaves aquadest extract. *Dent J: Majal. Ked. Gig.*, 46(1):9–13.
20. Lara, H. H., Ayala-Núñez, N. V., Turrent, L. del C. I., Padilla, C. R. (2010). Bactericidal effect of silver nanoparticles against multidrug-resistant bacteria. *World J. Microbiol. Biotechnol.*, 26(4):615–621.
21. Patra, J. K., Baek, K. -H. (2017). Antibacterial activity and synergistic antibacterial potential of biosynthesized silver nanoparticles against foodborne pathogenic bacteria along with its anticandidal and antioxidant effects. *Front. Microbiol.*, 8:167.
22. Yuan, Y. -G., Peng, Q. -L., Gurunathan, S. (2017). Effects of silver nanoparticles on multiple drug-resistant strains of *Staphylococcus aureus* and *Pseudomonas aeruginosa* from mastitis-infected goats: An alternative approach for antimicrobial therapy. *Int. J. Mol. Sci.*, 18(3):569.
23. Cohen-Karni, T., Langer, R., Kohane, D. S. (2012). The smartest materials: The future of nano electronics in medicine, *ACS Nano*, 6(8):6541–6545.
24. Dakal, T. C., Kumar, A., Majumdar, R. S., Yadav, V. (2016). Mechanistic Basis of Antimicrobial Actions of Silver Nanoparticles, *Front. Microbiol.*, 7:1831.
25. Escárcega-González, C. E., Garza-Cervantes, J., Vázquez-Rodríguez, A., Montelongo-Peralta, L. Z., Treviño-González, M., Castro, E. D. B., Saucedo-Salazar, E., Morales, R. C., Soto, D. R., González, F. T. (2018). In vivo

- antimicrobial activity of silver nanoparticles produced via a green chemistry synthesis using *Acacia Rigidula* as reducing and capping agent. *Int. J. Nanomed.*, 13:2349.
26. Mohammed, A. E., Al-Qahtani, A., Al-Mutairi, A., Al-Shamri, B., Aabed, K. (2018). Antibacterial and cytotoxic potential of biosynthesized silver nanoparticles by some plant extracts. *Nanomat.*, 8(6):382.
 27. Loo, Y.Y., Rukayadi, Y., Mahmud-Ab-Rashid Nor-Khaizura, C., Kuan, H., Chieng, B. W., Nishibuchi, M., Radu, S. (2018). In vitro antimicrobial activity of green synthesized silver nanoparticles against selected gram-negative foodborne pathogens. *Front. Microbiol.*, 9:1555.
 28. Venkatesan, J., Singh, S. K., Anil, S., Kim, S. -K., Shim, M. S. (2018). Preparation, characterization and biological applications of biosynthesized silver nanoparticles with chitosan-fucoidan coating. *Molecules*, 23(6):1429.
 29. Rai, M., Deshmukh, S., Ingle, A., Gade, A. (2012). Silver nanoparticles: the powerful nanoweapon against multidrug-resistant bacteria. *J. Appl. Microbiol.*, 112(5):841–852.
 30. Abdelmoteleb, A., Valdez-Salas, B., Ceceña-Duran, C., Tzintzun-Camacho, O., Gutiérrez-Miceli, F., Grimaldo-Juarez, O., González-Mendoza, D. (2017). Silver nanoparticles from *Prosopis glandulosa* and their potential application as biocontrol of *Acinetobacter calcoaceticus* and *Bacillus cereus*. *Chem. Spec. Bioavail.*, 29(1):1–5.
 31. Song, K. C., Lee, S. M., Park, T. S., Lee, B. S. (2009). Preparation of colloidal silver nanoparticles by chemical reduction method. *Kor. J. Chem. Eng.*, 26(1):153–155.
 32. Abbasi, E., Milani, M., Fekri Aval, S., Kouhi, M., Akbarzadeh, A., Tayefi Nasrabadi, H., Nikasa, P., Joo, S. W., Hanifehpour, Y., Nejati-Koshki, K. (2016). Silver Nanoparticles: Synthesis Methods, Bio-Applications and Properties. *Crit. Rev. Microbiol.*, 42(2):173–180.
 33. Goudarzi, M., Mir, N., Mousavi-Kamazani, M., Bagheri, S., Salavati-Niasari, M. (2016). Biosynthesis and characterization of silver nanoparticles prepared from two novel natural precursors by facile thermal decomposition methods. *Sci. Rep.*, 6:2539.
 34. Nasretidinova, G., Fazleeva, R., Osin, Y. N., Gubaidullin, A., Yanilkin, V. (2017). Methylviologen-mediated electrochemical synthesis of silver nanoparticles via reduction of agcl nanospheres stabilized by cetyltrimethylammonium chloride. *Rus. J. Electrochem.*, 53(1):25–38.
 35. Francis, S., Joseph, S., Koshy, E. P., Mathew, B. (2018). Microwave assisted green synthesis of silver nanoparticles using leaf extract of *Elephantopus Scaber* and its environmental and biological applications. *Art. Cell. Nanomed. Biotech.*, 46(4):795–804.
 36. Mehmood, A., Murtaza, G., Bhatti, T. M., Kausar, R. (2014). Enviro-friendly synthesis of silver nanoparticles using *Berberis lycium* leaf extract and their antibacterial efficacy. *Acta Metal. Sin. (Eng. Lett.)*, 27(1):75–80.
 37. Gomathi, M., Rajkumar, P., Prakasam, A., Ravichandran, K. (2017). Green synthesis of silver nanoparticles using *Datura stramonium* leaf extract and assessment of their antibacterial activity. *Res. Eff. Tech.*, 3(3), 280–284.
 38. Jain S., Mehata M. S. (2017). Medicinal plant leaf extract and pure flavonoid mediated green synthesis of silver nanoparticles and their enhanced antibacterial property. *Sci. Rep.*, 7(1):15867.
 39. Mittal, J., Jain, R., Sharma, M. M. (2017). Phytofabrication of silver nanoparticles using aqueous leaf extract of *Xanthium strumerium* l. and their bactericidal efficacy. *Adv. Nat. Sci.: Nanosci. Nanotech.*, 8(2):025011.
 40. Abirami A., Nagarani G., Siddhuraju P. (2014). The medicinal and nutritional role of underutilized citrus fruit *Citrus hystrix* (kaffir lime): A review. *Drug Inv. Tod.*, 6(1):1-5.
 41. Singh A., Gupta R., Tandon S., Pandey R. (2018). Anti-biofilm and anti-virulence potential of 3, 7-dimethyloct-6-enal derived from *Citrus hystrix* against bacterial blight of rice caused by *Xanthomonas oryzae* pv. *Oryzae*. *Microb. Pathogen.*, 115:264-271.
 42. Wongsariya K., Phanthong P., Bunyapraphatsara N., Srisukh V., Chomnawang M. T. (2014). Synergistic interaction and mode of action of *Citrus hystrix* essential oil against bacteria causing periodontal diseases. *Pharm. Biol.* 52(3), 273-280.
 43. Rekha C., Poornima G., Manasa M. (2012). Ascorbic acid, total phenol content and antioxidant activity of fresh juices of four ripe and unripe citrus fruits. *Chem. Sci. Trans.*, 1(2), 303-310.
 44. Veerasamy, R., Xin, T. Z., Gunasagaran, S., Xiang, T. F. W., Yang, E. F. C., Jeyakumar, N., Dhanaraj, S. A. (2011). Biosynthesis of silver nanoparticles using *Mangosteen* leaf extract and evaluation of their antimicrobial activities, *J. Saudi Chem. Soci.*, 15(2), 113–120.
 45. Ravichandran, V., Vasanthi, S., Shalini, S., Shah, S. A. A., Harish, R. (2016). Green synthesis of silver nanoparticles using *Atrocarpus atilis* leaf extract and the study of their antimicrobial and antioxidant activity. *Mat. Lett.*, 180:264–267.
 46. Wang, C., Mathiyalagan, R., Kim, Y. J., Castro-Aceituno, V., Singh, P., Ahn, S., Wang, D., Yang, D. C. (2016). Rapid green synthesis of silver and gold nanoparticles using *Dendropanax morbifera* leaf extract and their anticancer activities. *Int. J. Nanomed.*, 11:3691-701.
 47. Saxena, J., Sharma, P. K., Sharma, M. M., Singh, A. (2016). Process optimization For green synthesis of silver nanoparticles by *Sclerotinia sclerotiorum* MTCC 8785 and evaluation of its antibacterial properties. *SpringerPlus*, 5(1):861.
 48. Shittu K., Ihebunna O. (2017). Purification of simulated waste water using green synthesized silver nanoparticles of *Piliostigma thonningii* aqueous leave extract. *Adv. Nat. Sci.: Nanosci. Nanotech.*, 8(4):045003.
 49. Logeswari P, Silambarasan S., Abraham J. (2013). Ecofriendly synthesis of silver nanoparticles from commercially available plant powders and their antibacterial properties. *Sci. Iran.*, 20(3):1049–1054.
 50. Anandalakshmi K., Venugobal J., Ramasamy V. (2016). Characterization of silver nanoparticles by green synthesis method using *Petalium murex* leaf extract and their antibacterial activity. *Appl. Nanosci.*, 6(3):399–408.

51. Banala, R. R., Nagati, V. B., Karnati, P. R. (2015). Green synthesis and characterization of *carica papaya* leaf extract coated silver nanoparticles through x-ray diffraction, electron microscopy and evaluation of bactericidal properties. *Saudi J. Biol. Sci.*, 22(5):637–644.
52. Shaik, M. R., Khan, Mujeeb, Kuniyil, M., Al-Warthan, A., Alkathlan, H. Z., Siddiqui, M. R. H., Shaik, J. P., Ahamed, A., Mahmood, A., Khan, M. (2018). Plant-extract-assisted green synthesis of silver nanoparticles using *origanum vulgare* extract and their microbicidal activities. *Sustainability*, 10(4):913.
53. Ovais, M., Khalil, A. T., Raza, A., Khan, M. A., Ahmad, I., Islam, N. U., Saravanan, M., Ubaid, M. F., Ali, M., Shinwari, Z. K. (2016). Green synthesis of silver nanoparticles via plant extracts: beginning a new era in cancer theranostics. *Nanomed.*, 12(23):3157–3177.
54. Erjaee, H., Rajaian, H., Nazifi, S. (2017). Synthesis and characterization of novel silver nanoparticles using *Chamaemelum nobile* extract for antibacterial application. *Advances in Natural Sciences: Nanosci. Nanotech.*, 8(2):025004.
55. Sato A., Asano K., Sato T. (1990). The chemical composition of *Citrus hystrix* DC (swangi), *J. Essen. Oil Res.*, 2(4):179–183.
56. Deljou, A., Goudarzi, S. (2016). Green extracellular synthesis of the silver nanoparticles using *Thermophilic bacillus* sp. AZ1 and its antimicrobial activity against several human pathogenetic bacteria. *Iran. J. Biotech.*, 14(2):25–32.
57. Ashraf J. M., Ansari M. A., Khan H. M., Alzohairy M. A., Choi I. (2016). Green synthesis of silver nanoparticles and characterization of their inhibitory effects on AGEs formation using biophysical techniques. *Sci. Rep.*, 6:20414.
58. Dakhil A. S., Biosynthesis of silver nanoparticle (AgNPs) using *Lactobacillus* and their effects on oxidative stress biomarkers in rats. *J. King Saud. Univ. Sci.*, 29(4):462–467.
59. Jyoti, K., Baunthiyal, M., Singh, A. (2016). Characterization of silver nanoparticles synthesized using *Urtica dioica* Linn. leaves and their synergistic effects with antibiotics. *J. Radiat. Res. Appl. Sci.*, 9(3):217–227.
60. Yan, X., He, B., Liu, L., Qu, G., Shi, J., Hu, L., Jiang, G. (2018). Antibacterial mechanism of silver nanoparticles in *Pseudomonas aeruginosa*: proteomics approach. *Metallomics.*, 10(4):557–564.
61. Gurunathan, S., Choi, Y. -J., Kim, J. -H. (2018). Antibacterial efficacy of silver nanoparticles on endometritis caused by *Prevotella melaninogenica* and *Arcanobacterium pyogenes* in dairy cattle. *Int. J. Mol.*, 19(4):E1210.
62. Kim, D. H., Park, J. C., Jeon, G. E., Kim, C. S., Seo, J. H. (2017). Effect of the size and shape of silver nanoparticles on bacterial growth and metabolism by monitoring optical density and fluorescence intensity. *Biotechnol. Bioprocess Eng.*, 22(2):210–217.
63. Pazos-Ortiz, E., Roque-Ruiz, J. H., Hinojos-Márquez, E. A., López-Esparza, J., Donohué-Cornejo, A., Cuevas-González, J. C., Espinosa-Cristóbal, L. F., Reyes-López, S. Y. (2017). Dose-dependent antimicrobial activity of silver nanoparticles on polycaprolactone fibers against gram-positive and gram-negative bacteria. *J. Nanomater.*, 2017(6):1–9.
64. Emmanuel, R., Palanisamy, S., Chen, S. -M., Chelladurai, K., Padmavathy, S., Saravanan, M., Prakash, P., Ali, M. A., Al-Hemaid, F. M. (2015). Antimicrobial efficacy of green synthesized drug blended silver nanoparticles against dental caries and periodontal disease-causing microorganisms. *Mater. Sci. Eng. C.*, 56:374–379.

CITATION OF THIS ARTICLE

Fuloria S, Fuloria NK, Yi CJ, Khei TM, Joe TA, Wei LT, Sundram KM, Kathiresan S. Green Synthesis of Silver Nanoparticles Blended With *Citrus Hystrix* Fruit Juice Extract And Their Response To Periodontitis Triggering Microbiota. *Bull. Env. Pharmacol. Life Sci.*, Vol 8 [5] June 2019: 112-123